Physics in Medicine & Biology

PAPER • **OPEN ACCESS**

High-frequency SiPM readout advances measured coincidence time resolution limits in TOF-PET

To cite this article: Stefan Gundacker *et al* 2019 *Phys. Med. Biol.* **64** 055012

IOP Publishing Phys. Med. Biol. 64 (2019) 055012 (9pp) https://doi.org/10.1088/1361-6560/aafd52

Physics in Medicine & Biology

IPEM Institute of Physics and Engineering in Medicine

RECEIVED
25 October 2018

REVISED
10 December 2018

ACCEPTED FOR PUBLICATION
10 January 2019

PUBLISHED
26 February 2019

PAPER

High-frequency SiPM readout advances measured coincidence time resolution limits in TOF-PET

Stefan Gundacker[1,2], **Rosana Martinez Turtos**[2], **Etiennette Auffray**[2], **Marco Paganoni**[1] and **Paul Lecoq**[2]

[1] UniMIB, Piazza dell'Ateneo Nuovo, 1—20126, Milano, Italy
[2] CERN, 1211 Geneve 23, Switzerland

E-mail: stefan.gundacker@cern.ch

Keywords: high-frequency electronics, TOF-PET, LSO:Ce codoped with Ca, fast timing, coincidence time resolution, single photon time resolution, Cherenkov emission in scintillators

Abstract

Scintillator based radiation detectors readout by SiPMs successively break records in their reached time resolution. Nevertheless, new challenges in time of flight positron emission tomography (TOF-PET) and high energy physics are setting unmatched goals in the 10 ps range. Recently it was shown that high frequency (HF) readout of SiPMs significantly improves the measured single photon time resolution (SPTR), allowing to evaluate the intrinsic performance of large area devices; e.g. FBK NUV-HD SiPMs of 4×4 mm^2 area and 40 μm single photon avalanche diode (SPAD) size achieve 90 ps FWHM. In TOF-PET such readout allows to lower the leading edge detection threshold, so that the fastest photons produced in the crystal can be utilized. This is of utmost importance if a high SPTR and prompt Cherenkov light generated by the hot-recoil electron upon 511 keV photo-absorption should improve timing. This paper shows that high-frequency bipolar transistor readout of state-of-the-art SiPMs coupled to high-performance scintillators can substantially improve the best achievable coincidence time resolution (CTR) in TOF-PET. In this context a CTR of 158 ± 3 ps FWHM with $2 \times 2 \times 3$ mm^3 BGO crystals coupled to FBK SiPMs is achieved. This faint Cherenkov signal is as well present in standard LSO scintillators, which together with low SPTR values (<90 ps FWHM) improves the CTR of $2 \times 2 \times 3$ mm^3 LSO:Ce:Ca coupled to FBK NUV-HD 4×4 mm^2 with 25 μm SPAD size to 61 ± 2 ps FWHM using HF-electronics, as compared to 73 ± 2 ps when readout by the NINO front-end ASIC. When coupling the LSO:Ce:Ca crystals to FBK NUV-HD SiPMs of 4×4 mm^2 and 40 μm SPAD size, using HF-electronics, a CTR of even 58 ± 3 ps for $2 \times 2 \times 3$ mm^3 and 98 ± 3 ps for $2 \times 2 \times 20$ mm^3 is achieved. This new experimental data will allow to further discuss the timing limits in scintillator-based detectors.

List of acronyms

ASIC	Application-specific integrated circuit
BGO	$Bi_4Ge_3O_{12}$
CTR	Coincidence time resolution
FBK	Fondazione Bruno Kessler
FWHM	Full width at half maximum
HF	High-frequency
HPK	Hamamatsu Photonics K.K.
ILY	Intrinsic light yield
LSO	Lu_2SiO_5
LTE	Light transfer efficiency
LuAG	$Lu_3Al_5O_{12}$
LYSO	$(Lu,Y)_2SiO_5$
MMIC	Monolithic microwave integrated circuit

NUV-HD	Near ultraviolet high density
PDE	Photon detection efficiency
PMT	Photomultiplier tube
PTS	Photon transfer time spread
RF	Radio frequency
SiPM	Silicon photomultiplier
SPAD	Single photon avalanche diode
SPTR	Single photon time resolution
TOF-PET	Time of flight positron emission tomography

1. Introduction

Emerging challenges in time of flight positron emission tomography (TOF-PET) set the coincidence time resolution (CTR) goal towards values of 10 ps FWHM. In previous work we have concluded that there is no physical barrier prohibiting such low CTR values in PET (Gundacker 2014, Gundacker *et al* 2016b, Lecoq 2017). However, sound technological solutions have to be found in order to improve the photostatistics of the scintillation process (higher light yield, faster rise- and decay times) and the single photon time resolution (SPTR) of the photodetector, e.g. silicon photomultiplier (SiPM). Furthermore a complete assessment of the various available scintillators in terms of their best achievable time resolution is still missing. This is important, because the appearance of new photodetectors and readout electronics makes it successively possible to explore fast known and unknown scintillation processes. For example recent studies have shown that using Cherenkov emission in BGO upon 511 keV photo-absorption can deliver CTRs in the range of 200 ps FWHM (Brunner and Schaart 2017). Considering standard scintillation statistics, several publications (Hyman *et al* 1964, Conti *et al* 2009, Seifert *et al* 2012b, Gundacker *et al* 2013a, Derenzo *et al* 2014) conclude that the CTR is directly proportional to the square root of the scintillation decay time (τ_d) and indirectly proportional to the square root of the number of detected photons (n'), i.e. CTR $\propto \sqrt{\tau_d/n'}$. If further only scintillation statistics is considered the CTR would be as well directly proportional to the square root of the scintillation rise time τ_r, as shown in equation (1). The factor 2.18 is a consequence of determining the variance of the first scintillation photon emitted and includes the transformation into FWHM of the standard deviation in coincidence (Gundacker 2014, Gundacker *et al* 2016b).

$$\mathrm{CTR}_{1^{st}} = 2.18 \cdot \sqrt{\frac{\tau_r \cdot \tau_d}{n'}}. \tag{1}$$

Equation (1) already gives a good idea of the intrinsic time resolution limit of scintillator based detectors. For example if considering LYSO:Ce with an intrinsic light yield of 20 500 photons per 511 keV (Turtos *et al* 2016), a rise time of 70 ps and a decay time of 40 ns (Gundacker *et al* 2016b) the $\mathrm{CTR}_{1^{st}} = 25$ ps. Lowering the rise time to 20 ps and the decay time to 30 ns in the case of LSO:Ce:Ca would lower this value to $\mathrm{CTR}_{1^{st}} = 12$ ps FWHM. This shows that the scintillation statistics itself would allow for very good CTRs, however, inefficiencies in the detector like additional photon time transfer spread (PTS) and imperfect light transfer efficiency (LTE) of the emitted scintillation light deteriorates the best achievable time resolution (Derenzo *et al* 2014, Gundacker *et al* 2014). As well the electronic readout can potentially degrade the CTR. This influence was estimated to be low or even negligible in past studies (Gundacker *et al* 2013a), however, the appearance of SiPMs with very good single photon time resolutions (<90 ps FWHM) demand to re-evaluate this statement. Indeed, measurements presented in this work will show that a significant improvement in CTR can be achieved if HF electronic readout of high-performance SiPMs with high SPTR is being used.

2. Materials and methods

This section gives an overview of the crystals and SiPMs utilized in this study, followed by a depiction of the CTR measurement setup. Special attention is given to the introduction of the high-frequency readout electronics and its comparison to the well established NINO front-end ASIC (Anghinolfi *et al* 2004). These two electronic readout concepts are further discussed within SPTR measurements, giving a first insight in the combined SiPM—electronic performance.

2.1. LSO:Ce codoped Ca scintillators and FBK NUV-HD SiPMs

For our studies we used $2 \times 2 \times 3$ mm^3 sized LSO:Ce codoped with 0.4%Ca and $2 \times 2 \times 20$ mm^3 sized LSO:Ce codoped with 0.2%Ca crystals from the producer Agile. Both scintillation materials show very fast decay and rise times (Gundacker *et al* 2018), whereas the self absorption is a bit less in the 0.2%Ca codoped crystals making them better suitable for higher aspect ratios (Gundacker *et al* 2016). The scintillation properties of both materials are summarized in table 1.

Table 1. Measured scintillation kinematics of the scintillators used in this study. The intrinsic light yield (ILY) of the LSO:Ce:Ca samples was estimated by light output measurements of $2 \times 2 \times 10$ mm^3 crystals relative to LYSO:Ce crystals with the same dimensions. The ILY of this LYSO:Ce was afore determined to 40 000 ph MeV^{-1} by electron excitation (Turtos *et al* 2016). The measurements were performed with a Hamamatsu PMT R2059, crystals were wrapped in Teflon and optically coupled by Rhodorsil 47 V ($n = 1.42$). For further information we refer to Gundacker *et al* (2016) and Gundacker *et al* (2018).

Composition	τ_r (ps)	τ_{d1} (ns)	R_1 (%)	τ_{d2} (ns)	R_2 (%)	ILY (ph MeV^{-1})
LSO:Ce:0.2%Ca	9 ± 9	10.8 ± 1	5 ± 1	35.0 ± 0.2	95 ± 1	39 200
LSO:Ce:0.4%Ca	10 ± 10	7.5 ± 1	5 ± 1	32.4 ± 0.2	95 ± 1	32 000

As photodetectors we used two different near ultraviolet high density (NUV-HD) SiPMs with an active area of 4×4 mm^2 and 25×25 μm^2 or 40×40 μm^2 single photon avalanche diode (SPAD) size from Fondazione–Bruno–Kessler (FBK) (Piemonte *et al* 2016). These SiPMs exhibit a very high fill factor which allows for peak photon detection efficiency (PDE) values of up to 55%–65% at 410 nm (Piemonte *et al* 2016) and because of no entrance window (for these particular samples) a direct coupling to the bare SiPM with high refractive index glues is possible (in this work Meltmount with refractive index of $n = 1.582$). We estimate the product of PDE and LTE, i.e. the fraction of light produced in the scintillator which is detected by the SiPM, roughly to be in the order of ~44% in the case of $2 \times 2 \times 3$ mm^3 and ~24% in the case of $2 \times 2 \times 20$ mm^3 crystals. The PDE as well extents to the near ultraviolet (>35% for 300 nm) making them perfect candidates to sense Cherenkov (Lecoq *et al* 2010, Brunner *et al* 2014, Kwon *et al* 2016) and hot intraband (Omelkov *et al* 2016, 2018) emission produced in the scintillator. Additionally, these SiPMs show best single photon time resolution (SPTR) as compared to other producers with measured values of 90 ps FWHM when illuminating the whole device (Cates *et al* 2018). Subtracting the laser pulse width of 42 ps FWHM (Nemallapudi *et al* 2016) and the remaining electronic noise term of 35 ps FWHM, the intrinsic SPTR of the whole device illuminated is 71 ps FWHM. We have measured the breakdown voltage of the 25×25 μm^2 SPAD area SiPM to 25.4 V and of the 40×40 μm^2 to 28.2 V.

2.2. Electronics: high frequency readout

In figure 1(a) we show the HF amplifier schematics used in this study. The HF part with the transformer was already introduced in Cates *et al* (2018), although in the present work different RF-amplifiers are used, i.e. BGA616. The implemented transmission line transformer is commercially available (Macom MABA-007159) with a cut-off frequency of 3 GHz and small dimensions of $3.81 \times 3.81 \times 2.6$ mm^3 only. This circuit efficiently amplifies and extracts the high-speed high bandwidth signal from the SiPM which is mainly coupled via the quenching capacitance C_D of the SPAD to the SiPM output terminal (Corsi *et al* 2006, Seifert *et al* 2009). It should be noted that the SiPM terminal capacitance (the capacitance of the inactive cells plus the SiPM grid capacitance) together with the quenching capacitance C_D constitutes a capacitive divider for the fast SPAD signal. Hence, in this readout-scheme a larger SiPM area and thus higher terminal capacitance implicates a measured lower amplitude of the single photon avalanche signal. The bandwidth of the HF-signal path was measured to be approximately 1.5 GHz when the SiPM is connected to the amplifier. Because the voltage amplification of the HF-part is between 50 and 100 (depending on the applied amplifier bias current) a second path to measure the energy deposited in the crystal glued to the SiPM is needed. This was realized with a standard AD8000 operational amplifier circuit which does not significantly lower the timing channel bandwidth nor introduces additional electronic noise. The particular advantage of splitting the energy and time signal allows to have the best resolution for the timing and energy channels independently. For comparison we show in figure 1(b) the schematics of the SiPM readout with the NINO front-end ASIC (Anghinolfi *et al* 2004, Gundacker *et al* 2013a). Figure 2(a) shows an example of the measured SPTR with FBK NUV-HD SiPMs having a 4×4 mm^2 active area and 40 μm SPAD pitch, using the NINO front-end ASIC or this HF-amplifier. As already mentioned with this HF-amplifier it is possible to measure SPTR values of 90 ps FWHM illuminating the whole 4×4 mm^2 FBK SiPM, due to its high-bandwidth allowing for highest slew rates (Cates *et al* 2018). This means a real intrinsic SPTR of 71 ps FWHM subtracting the laser pulse width of 42 ps FWHM and the remaining electronic noise part of 35 ps FWHM. In figure 2(b) we additionally show the measured SPTR for Hamamatsu S13360 SiPMs with 3×3 mm^2 active area and 50 μm SPAD size. Here the improvement achieved by the HF readout as compared to NINO is less pronounced. This can be explained by a higher SPAD signal amplitude for the HPK sample in regard to the FBK NUV-HD SiPM (~2 times) due to the smaller SiPM area and larger SPAD size, hence, the electronic noise influence is less pronounced for the NINO measurements. The overall higher SPTR for HPK might be explained by a worse intrinsic time resolution of the SPADs themselves caused by a different electric field configuration in the SPAD leading to stronger edge effects (Acerbi and Gundacker 2018). The SPTR measurements have been performed with a PiLas picosecond laser at a wavelength of 420 nm. More details for NINO measurements can be found in Nemallapudi *et al* (2016) and for HF-amplifer measurements in Cates *et al* (2018).

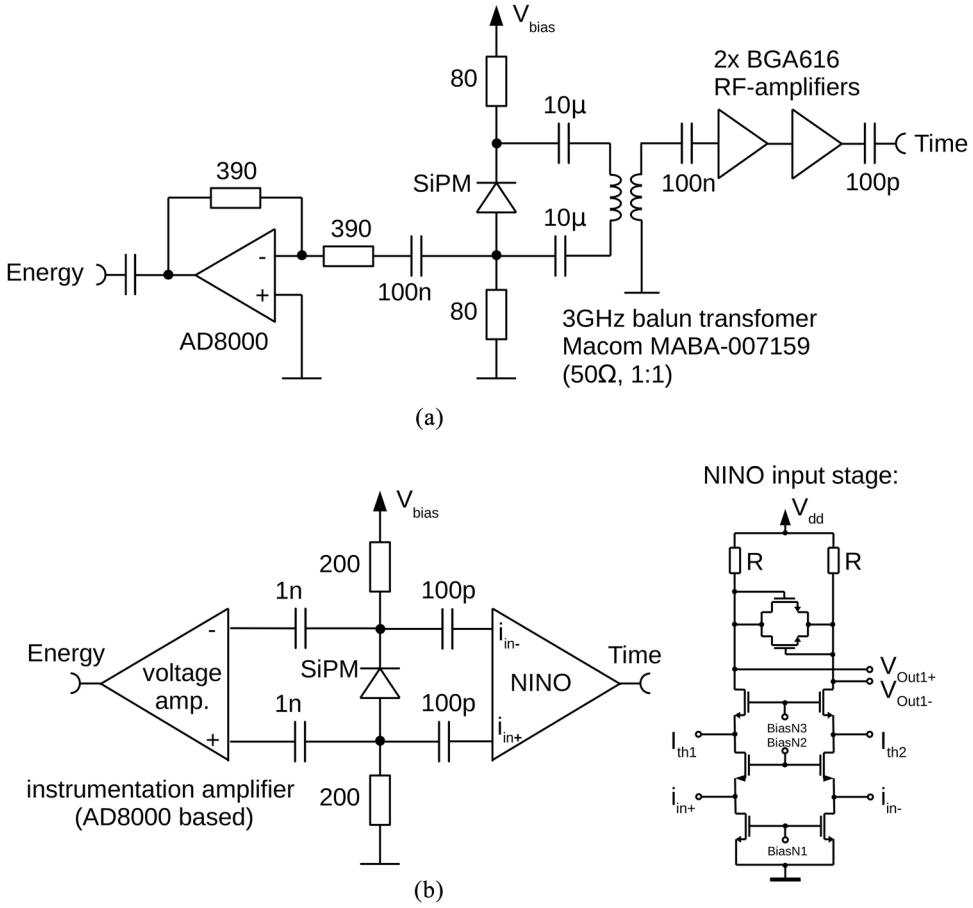

Figure 1. (a) Schematics of the HF-amplifier readout electronics employing two BGA616 bipolar monolithic microwave integrated circuit (MMIC) amplifiers. (b) Schematics of the readout electronics using the time-over-threshold discriminator chip NINO. The input stage of NINO is as well shown on the right hand side (Anghinolfi *et al* 2004).

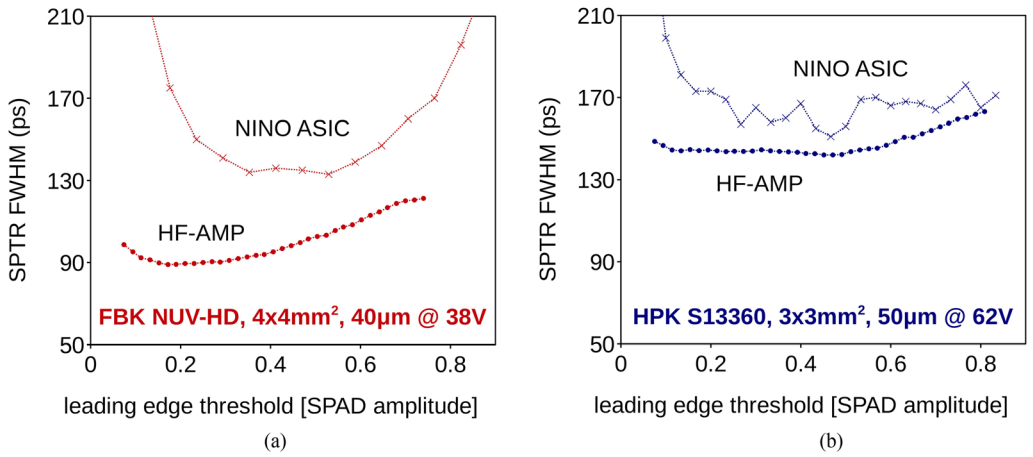

Figure 2. (a) The SPTR measured with the HF-amplifier is significantly better as compared to the measured SPTR with NINO for FBK NUV-HD SiPMs with 4×4 mm^2 active area and 40 μm SPAD size. This can be understood by a suppressed electronic noise term due to a very high slew rate (dV/dt) of the HF-amplifier signal. SiPM operated at 9.8V overvoltage. (b) SPTR values measured with HPK S13360, 3×3 mm^2 area and 50 μm SPAD size with the HF-electronics and NINO readout. The SPTR improvement using HF-electronics is less pronounced because of a higher single photo-electron signal amplitude seen in this HPK SiPM (larger SPAD size, smaller SiPM area). SiPM operated at 10.5 V overvoltage.

2.3. Coincidence time resolution measurement setup

The CTR was measured with the standard setup shown in figure 3(a). A ^{22}Na source emits two 511 keV gammas which are detected in coincidence by the LSO:Ce:Ca crystals coupled to the NUV-HD SiPMs readout by the HF-electronics for the time signal and the analog operational amplifier for the energy signal. The electronic signals are digitized by a LeCroy DDA735Zi oscilloscope with 3.5 GHz bandwidth and a sampling rate of 40 Gs s^{-1}

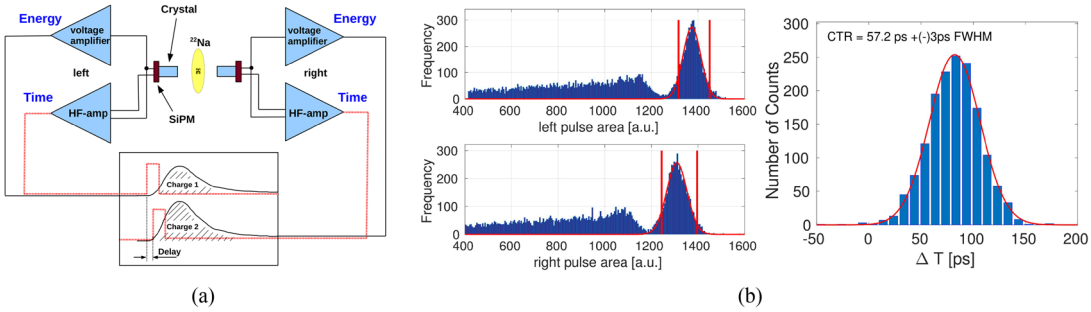

Figure 3. (a) In the CTR setup we readout the energy signal separately from the time signal to maintain highest time and energy resolution. (b) Example of measured energy spectra and photopeak selection with resulting delay time histogram and Gaussian fit giving the CTR in FWHM.

(using four channels this reduces to 20 Gs s^{-1}, i.e. 50 ps binning). The leading edge threshold is set on the oscilloscope calculating the signal crossing time via linear interpolation. In figure 3(b) an example of the energy spectra recorded is shown together with the applied photopeak selection (-1.5σ, $+2\sigma$). It should be mentioned that the exact photopeak selection window is changing the obtained CTR marginally by a few picoseconds only. Plotting the delay times for the selected events gives the delay time histogram and a resulting Gaussian fit the CTR in full width at half maximum (FWHM). To test the acquisition system for nonlinearities, we also performed several scans that moved the source position by a known distance along the line of response and recorded the time offset of the delay time histogram. If not stated otherwise we always wrapped the crystals in Teflon (at least three layers) and glued them with Meltmount ($n = 1.582$) to the bare SiPM without protective glass or resin window.

3. Coincidence time resolution results

3.1. NUV-HD with 25 × 25 μm^2 SPADs coupled to 3 and 20 mm long LSO:Ce:Ca

In figure 4 the CTR measured with NUV-HD 25 × 25 μm^2 SPADs is shown for two crystal sizes (2 × 2 × 3 mm^3 and 2 × 2 × 20 mm^3) from the producer Agile. The measurements were performed at a SiPM bias voltage of 38 V (12.6 V overvoltage), which was determined to be the optimum for this SiPM (Gundacker *et al* 2016). The single SPAD amplitude at this overvoltage was measured to 28.6 mV applying maximum bandwidth (∼1.5 GHz). Additionally, figure 4(a) shows the effect of limiting the electronic bandwidth for the 3 mm long crystal coupled. Lowering the bandwidth from ∼1.5 GHz provided by the amplifier to 200 MHz deteriorates the CTR from 61 ± 2 ps to 70 ± 3 ps, respectively. In the exact same configuration we measured 73 ± 3 ps with the NINO front-end ASIC (Gundacker *et al* 2016), which most likely is explained by the lower bandwidth and speed of NINO as compared to this HF-amplifier. With 1 GHz bandwidth limit we measure a best CTR of 64 ± 2 ps FWHM, which is only slightly but nevertheless significantly worse than with the full bandwidth of ∼1.5 GHz. This measured worse CTR with lower electronic bandwidth can be understood by a slower signal slew rate and additional averaging of the detected time stamps due to the bandwidth filtering which obscures the time information of the first photons detected, as well seen by a minimum CTR at higher threshold values. To check our setup and to exclude any bias in the experiment we show in figure 4(b) measurements done with different source positions. As expected the centroid of the Gaussian is moving by ∼6.67 ps per each millimeter of source displacement.

3.2. NUV-HD with 40 × 40 μm^2 SPADs coupled to 3 and 20 mm LSO:Ce:Ca

CTR measurements performed with NUV-HD 40 × 40 μm^2 SPAD size are shown in figure 5. The values are measured at a SiPM bias of 39 V (10.8 V overvoltage), determined to give the best CTR values. At this overvoltage the single SPAD signal was measured to be 44.2 mV applying maximum bandwidth (∼1.5 GHz). For the long LSO:Ce:0.2%Ca 2 × 2 × 20 mm^3 crystal we obtain a best CTR of 98 ± 2 ps FWHM, constituting a significant improvement as compared to the 25 μm SPAD size SiPM, which we mainly explain by the higher PDE of the 40 μm SPAD SiPM. A CTR of 58 ± 2 ps FWHM is obtained in the case of coupling 2 × 2 × 3 mm^3 LSO:Ce:0.4%Ca to the 40 μm SPAD SiPM. Further, it can be seen that the highest CTR for 20 mm long crystals is achieved at somewhat higher thresholds (∼30 mV) as compared to 3 mm long crystals (∼10 mV). This is a direct consequence of the additional PTS in the longer crystal which sets the best timing at a higher rank of photon-detection (Fishburn and Charbon 2010, Seifert *et al* 2012a, Gundacker *et al* 2015). Furthermore we want to mention that the CTR results shown in figure 5(a) are performed with a longer measurement time, which is the reason for the smaller statistical fluctuation as compared to the CTR values presented in figure 4(a). CTR measurements with different source positions for the 20 mm long crystals can be seen in figure 5(b).

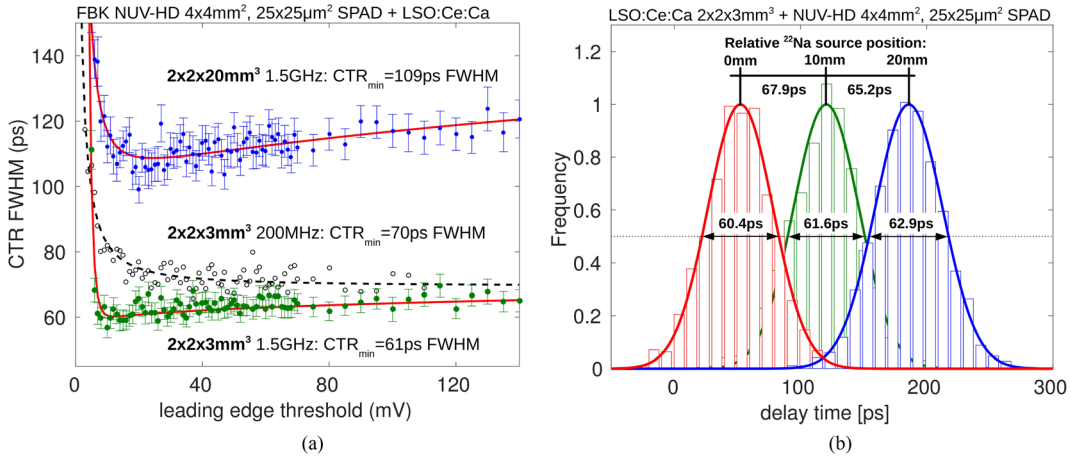

Figure 4. (a) Measured CTR as a funtion of leading edge threshold with $2 \times 2 \times 3$ mm^3 LSO:Ce:0.4%Ca and $2 \times 2 \times 20$ mm^3 LSO:Ce:0.2%Ca crystals coupled to FBK NUV-HD 4×4 mm^2 SiPMs with 25 μm SPAD size. Additionally the CTR with $2 \times 2 \times 3$ mm^3 crystal size is shown when the bandwidth of the timing signal is limited to 200 MHz (black circles and fit as black dotted line). (b) Source movement measurements of FBK NUV-HD 4×4 mm^2 SiPMs with 25 μm SPAD size coupled to $2 \times 2 \times 3$ mm^3 LSO:Ce:0.4%Ca crystals. The centroid of the Gaussian is moving as expected by $\sim$6.67 ps mm^{-1} if the ^{22}Na source is displaced, confirming a correct mode of operation. All measurements were performed at a SiPM bias of 38 V (12.6 V over breakdown). The single SPAD signal amplitude is 28.6 mV at full bandwidth of $\sim$1.5 GHz.

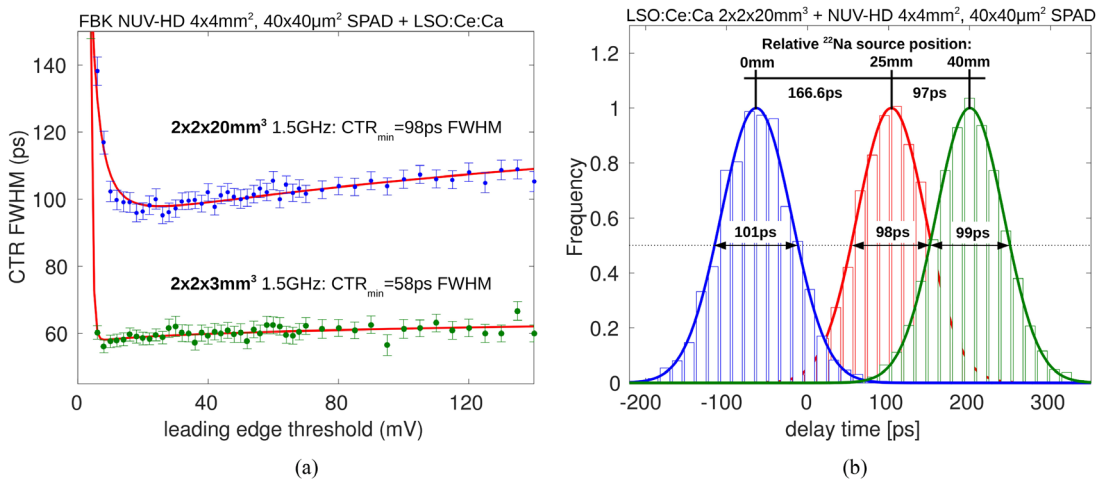

Figure 5. (a) Measured CTR as a function of leading edge threshold measured with $2 \times 2 \times 3$ mm^3 LSO:Ce:0.4%Ca and $2 \times 2 \times 20$ mm^3 LSO:Ce:0.2%Ca crystals coupled to FBK NUV-HD 4×4 mm^2 SiPMs with 40 μm SPAD size. (b) With the same setup when $2 \times 2 \times 20$ mm^3 LSO:Ce:0.2%Ca crystals are coupled, the centroid of the Gaussian delay time histogram is moving as expected by $\sim$6.67 ps mm^{-1} ^{22}Na displacement, confirming a correct mode of operation. All measurements were performed at a SiPM bias of 39 V (10.8 V over breakdown). The single SPAD amplitude is 44.2 mV at full bandwidth of $\sim$1.5 GHz.

3.3. The case of BGO and prompt photon emission

Due to the fast slew rate of the electronic signal delivered by the high-frequency readout it becomes as well possible to use the faint prompt photon emission (Cherenkov and hot intraband luminescence) in scintillators, e.g. in BGO or LuAG:Pr. An example of the measured CTR with BGO can be seen in figure 6 performed with FBK NUV-HD 4×4 mm^2, 40×40 μm^2 SPAD size coupled to $2 \times 2 \times 3$ mm^3 BGO wrapped in Teflon and coupled with Meltmount ($n = 1.582$). A best CTR of 158 ± 3 ps FWHM can be achieved being even better than comparable measurements stated in literature (Kwon *et al* 2016) or with the Philips digital SiPM (Brunner and Schaart 2017). Hence, in order to achieve a high CTR by prompt photon emission it is of utmost importance to be able to trigger on the very first photons detected. This can be seen in figure 6(a) where lowering the leading edge threshold rapidly leads to better timing until electronic noise prohibits a further decrease of the threshold. We as well observe in figure 6(b) that such low thresholds in large part suppresses long tails in the CTR histogram as compared to former studies (Brunner and Schaart 2017), implying that the time stamps are mostly generated by prompt photons and not the intrinsic BGO scintillation. This is further illustrated by figure 6(b) showing two fits, a standard Gaussian fit and a fit applying two overlapping Gaussians one accounting for the prompt photon emission statistics and the other for the BGO scintillation emission statistics. In this particular case (at a leading edge threshold of 10 mV) we obtain a FWHM of 137 ps for the prompt photon emission Gaussian with a relative abundance of 72% and a FWHM of 276 ps for the assumed BGO scintillation emission with a relative abundance of 28%.

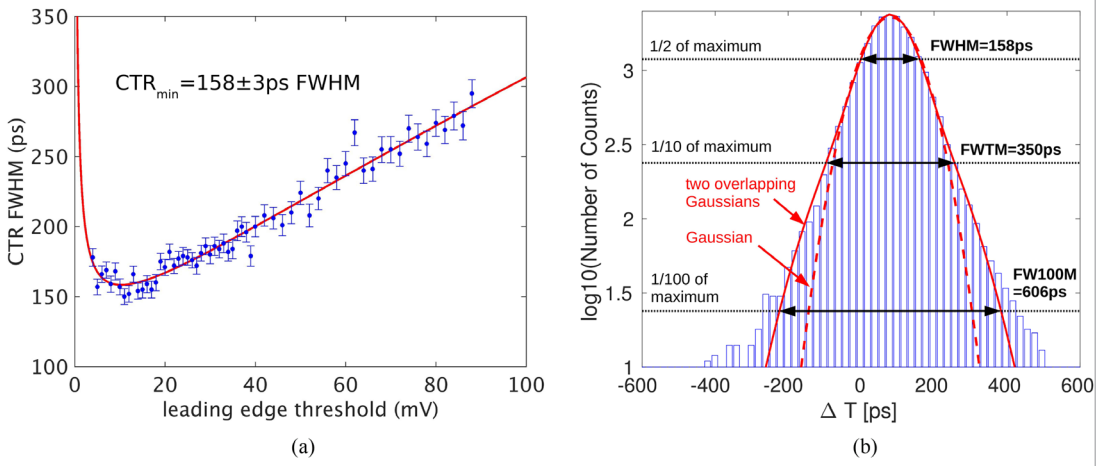

Figure 6. (a) Measured best CTR of 158 ps FWHM with $2 \times 2 \times 3$ mm^3 BGO coupled to NUV-HD 4×4 mm^2 SiPMs, 40 μm SPAD size. Only at very low leading edge thresholds this value can be achieved. (b) Delay time histogram measured at 10 mV leading edge threshold. Shown is a Gaussian fit to the data (dotted red line) and a fit of two overlapping Gaussians (solid red line)—Gaussian_1 with 137 ps FWHM and 72% relative abundance and Gaussian_2 with 276 ps FWHM and 28% relative abundance. The single SPAD amplitude is 44.2 mV for the applied 39 V SiPM bias (10.8 V overvoltage).

4. Discussing the SiPM readout

The best time resolution achieved by the electronic readout can be summarized with the relation $\sigma_{elec.\ timing} = \frac{\sigma_n}{dV/dt}$ (Nemallapudi *et al* 2016, Cates *et al* 2018) with the electronic noise given by the rms or standard deviation of the noise floor (σ_n) and the signal slew rate (dV/dt) of the signal at a given leading edge detection threshold. Hence, improving the electronic readout timing jitter can be done by increasing the signal amplitude, decreasing the signal rise time or lowering the electronic noise floor. The later has clear physical barriers and can only be improved by a limited amount. Interestingly SiPMs show a very fast intrinsic single photon signal rise time of the order of several hundreds of picoseconds (Acerbi and Gundacker 2018). To utilize this very fast signal rise time in order to achieve a high signal slew rate (dV/dt), high-frequency readout is necessary with a -3 dB bandwidth noticeably higher 1 GHz, with the detector (SiPM) coupled to the electronics. The discussed design in this paper employing an RF-balun transformer represents an efficient way to readout the SiPM signal in a differential mode adapting to the single ended input of high speed high-frequency monolithic microwave integrated circuit (MMIC) amplifiers (e.g. BGA616). This has two immediate advantages, suppressing common ground noise in the SiPM and doubling the signal amplitude at the amplifier input. As already discussed, via the quenching resistor's parallel capacitance (C_D) a high-frequency path is established allowing to use the intrinsically very fast SPAD signal rise time. A disadvantage of this design is that the SiPM voltage signal height depends on the terminal capacitance and, hence, is lower for larger area SiPMs. However, the use of transformers with adapted turn ratio could help to a certain extent in such situations.

In the current form the integration of this circuit into an ASIC with many channels is rather difficult. The main limiting factor besides the RF-transformer is the quite high power consumption of the MMIC amplifiers. Within a proper design the use of the RF-transformer could probably be omitted without significant performance loss, which will be subject for future studies. Reducing the power budget will as well lower the available bandwidth and thus decreases the signal slew rate. This is partly offset by a reduction in electronic noise due to the lower bandwidth design but still constitutes a worse situation, because the optimal electronic bandwidth is naturally linked to the intrinsic bandwidth (rise time) of the SiPM signal. Another way to improve timing without increasing the electronic bandwidth could be the symbiotic development of the SiPM plus readout ASIC. For instance by implementing ways to enhance the fast signal amplitude, e.g. increasing the quenching capacitance C_D or employing a specially designed fast readout node, as done in SensL devices (O'Neill *et al* 2012).

To conclude, high-frequency readout is one way to reach the limits in timing performance given by modern analog SiPMs, but most likely not the only way. On the other hand, the fully digital SiPM does not struggle with these limitations and will presumably be the best option to achieve the intrinsic timing limits in TOF-PET, given by photostatistics and the photodetector itself, if the detector can be successfully integrated in a scalable 3D design (Nolet *et al* 2018).

5. Conclusion

We have shown that HF readout with a −3 dB bandwidth ∼1.5 GHz of SiPMs can improve the timing in TOF-PET noticeably with CTR values measured of 58 ± 2 ps and 98 ± 3 ps for 2 × 2 × 3 mm^3 and 2 × 2 × 20 mm^3 LSO:Ce codoped with Ca crystals, respectively. The main reason of this improvement as compared to standard ASIC readout lies in a much faster signal slew rate (dV/dt) which allows to detect the very first photons sensed by the SiPM, i.e. the leading edge threshold can be lowered effectively in a greater extent. The current generation of NUV-HD SiPMs from FBK shows as well very low intrinsic SPTR values (<71 ps FWHM) and high photon detection efficiency in the near ultraviolet. These two factors additionally help to improve the CTR via (1) a high SPTR which allows to utilize the intrinsic high timing performance of the LSO:Ce:Ca scintillation process and (2) the ultraviolet sensitivity which increases the detection probability of prompt photons (in particularly Cherenkov radiation but as well to some extent hot intraband luminescence). Here it is important to mention that these two factors only can improve the CTR if a low leading edge threshold can be achieved. In other words, the HF-readout allows to make best use of the good SPTR of the tested SiPMs without deteriorating the CTR by a too high electronic noise or small slew rate. This again underlines the importance of a low SPTR value in SiPMs and the interplay of the electronic readout. In a large system, where power consumption limits do not allow for extremely high bandwidths other solutions have to be found, which can and have to be developed symbiotically with the SiPM design. Further studies in this direction and additional experiments to understand the full connection of prompt photons and the SPTR are ongoing and will be subject to future publications.

Acknowledgment

This work has been performed in the framework of the Crystal Clear Collaboration, COST Action TD1401 (FAST) and the TICAL ERC advanced grant #338953. The authors would like to express their highest gratitude to Joshua William Cates and Pierre Jarron for the many interesting and fruitful discussions. Further we want to thank Claudio Piemonte, Alberto Gola and the whole FBK team for kindly providing the SiPM samples used in this study.

ORCID iDs

Stefan Gundacker https://orcid.org/0000-0003-2087-3266
Rosana Martinez Turtos https://orcid.org/0000-0002-1077-4849

References

Acerbi F and Gundacker S 2018 Understanding and simulating SiPMs *Nucl. Instrum. Methods Phys. Res. A* accepted (https://doi.org/10.1016/j.nima.2018.11.118)
Anghinolfi F, Jarron P, Krummenacher F, Usenko E and Williams M 2004 NINO: aN ultrafast low-power front-end amplifier discriminator for the time-of-flight detector in the ALICE experiment *IEEE Trans. Nucl. Sci.* **51** 1974–8
Brunner S and Schaart D R 2017 BGO as a hybrid scintillator/Cherenkov radiator for cost-effective time-of-flight PET *Phys. Med. Biol.* **62** 4421–39
Brunner S E, Gruber L, Marton J, Suzuki K and Hirtl A 2014 Studies on the Cherenkov effect for improved time resolution of TOF-PET *IEEE Trans. Nucl. Sci.* **61** 443–7
Cates J W, Gundacker S, Auffray E, Lecoq P and Levin C S 2018 Improved single photon time resolution for analog SiPMs with front end readout that reduces influence of electronic noise *Phys. Med. Biol.* **63** 11
Conti M, Eriksson L, Rothfuss H and Melcher C L 2009 Comparison of fast scintillators with TOF PET potential *IEEE Trans. Nucl. Sci.* **56** 926–33
Corsi F *et al* 2006 Electrical characterization of silicon photo-multiplier detectors for optimal front-end design *IEEE NSS Conf. Record N30-222* pp 1276–80
Derenzo S E, Choong W and Moses W W 2014 Fundamental limits of scintillation detector timing precision *IOP Phys. Med. Biol.* **59** 3261–86
Fishburn M W and Charbon E 2010 System tradeoffs in gamma-ray detection utilizing SPAD arrays and scintillator *IEEE Trans. Nucl. Sci.* **57** 2549–56
Gundacker S 2014 Time resolution in scintillator based detectors for positron emission tomography *PhD Thesis* (Vienna University of Technology)
Gundacker S, Acerbi F, Auffray E, Gola A, Nemallapudi M, Paternoster G, Piemonte C and Lecoq P 2016 State of the art timing in TOF-PET detectors with LuAG, GAGG and L(Y)SO scintillators of various sizes coupled to FBK-SiPMs *J. Instrum.* **11** P08008
Gundacker S, Auffray E, Frisch B, Jarron P, Knapitsch A, Meyer T, Pizzichemi M and Lecoq P 2013a Time of flight positron emission tomography towards 100 ps resolution with L(Y)SO: an experimental and theoretical analysis *J. Instrum.* **8** P07014
Gundacker S, Auffray E, Jarron P, Meyer T and Lecoq P 2015 On the comparison of analog and digital SiPM readout in terms of expected timing performance *Nucl. Instrum. Methods Phys. Res.* A **787** 6–11
Gundacker S, Auffray E, Pauwels K and Lecoq P 2016b Measurement of intrinsic rise times for various L(Y)SO and LuAG scintillators with a general study of prompt photons to achieve 10 ps in TOF-PET *Phys. Med. Biol.* **61** 2802–37
Gundacker S, Knapitsch A, Auffray E, Jarron P, Meyer T and Lecoq P 2014 Time resolution deterioration with increasing crystal length in a TOF-PET system *Nucl. Instrum. Methods Phys. Res.* A **737** 92–100

Gundacker S, Turtos R M, Auffray E and Lecoq P 2018 Precise rise and decay time measurments of inorganic scintillators by means of x-ray and 511 keV excitation *Nucl. Instrum. Methods Phys. Res.* A **891** 42–52
Hyman L, Schwarcz R and Schluter R 1964 Study of high speed photomultiplier systems *Rev. Sci. Instrum.* **35** 393–406
Kwon S, Gola A, Ferri A, Piemonte C and Cherry S 2016 Bismuth germanate coupled to near ultraviolet silicon photomultipliers for time-of-flight PET *Phys. Med. Biol.* **61** L38–47
Lecoq P 2017 Pushing the limits in time-of-flight PET imaging *IEEE Trans. Radiat. Plasma Med. Sci.* **1** 476–85
Lecoq P, Auffray E, Brunner S, Hillemanns H, Jarron P, Knapitsch A, Meyer T and Powolny F 2010 Factors influencing time resolution of scintillators and ways to improve them *IEEE Trans. Nucl. Sci.* **57** 2411–6
Nemallapudi M, Gundacker S, Lecoq P and Auffray E 2016 Single photon time resolution of state of the art SiPMs *J. Instrum.* **11** P10016
Nolet F, Dubois F, Roy N, Parent S, Lemaire W, Massie-Godon A, Charlebois S A, Fontaine R and Pratte J F 2018 Digital SiPM channel integrated in CMOS 65 nm with 17.5 ps FWHM single photon timing resolution *Nucl. Instrum. Methods Phys. Res. A* **912** 29–32
Omelkov S, Nagirnyi V, Gundacker S, Spassky D A, Auffray E, Lecoq P and Kirm M 2018 Scintillation yield of hot intraband luminescence *J. Lumin.* **198** 260–71
Omelkov S, Nagirnyi V, Vasilev A and Kirm M 2016 New features of hot intraband luminescence for fast timing *J. Lumin.* **176** 309–17
O'Neill K, Pavlov N, Dolinsky S and Jackson C 2012 SensL new fast timing silicon photomultiplier *Proc. of Science PoS(PhotoDet 2012)022*
Piemonte C, Acerbi F, Ferri A, Gola A, Paternoster G, Regazzoni V, Zappala G and Zorzi N 2016 Performance of NUV-HD silicon photomultiplier technology *IEEE Trans. Electron. Dev.* **63** 1111–6
Seifert S, van Dam H, Huizenga J, Vinke R, Dendooven P, Löhner H and Schaart D R 2009 Simulation of silicon photomultiplier signals *IEEE Trans. Nucl. Sci.* **56** 3726–33
Seifert S, van Dam H T and Schaart D R 2012a The lower bound on the timing resolution of scintillation detectors *Phys. Med. Biol.* **57** 1797–814
Seifert S, van Dam H, Vinke R, Dendooven P, Löhner H, Beekman F and Schaart D 2012b A comprehensive model to predict the timing resolution of SiPM-based scintillation detectors: theory and experimental validation *IEEE Trans. Nucl. Sci.* **59** 190–204
Turtos R, Gundacker S, Pizzichemi M, Ghezzi A, Pauwels K, Auffray E, Lecoq P and Paganoni M 2016 Measurement of LYSO intrinsic light yield using electron excitation *IEEE Trans. Nucl. Sci.* **63** 475–9